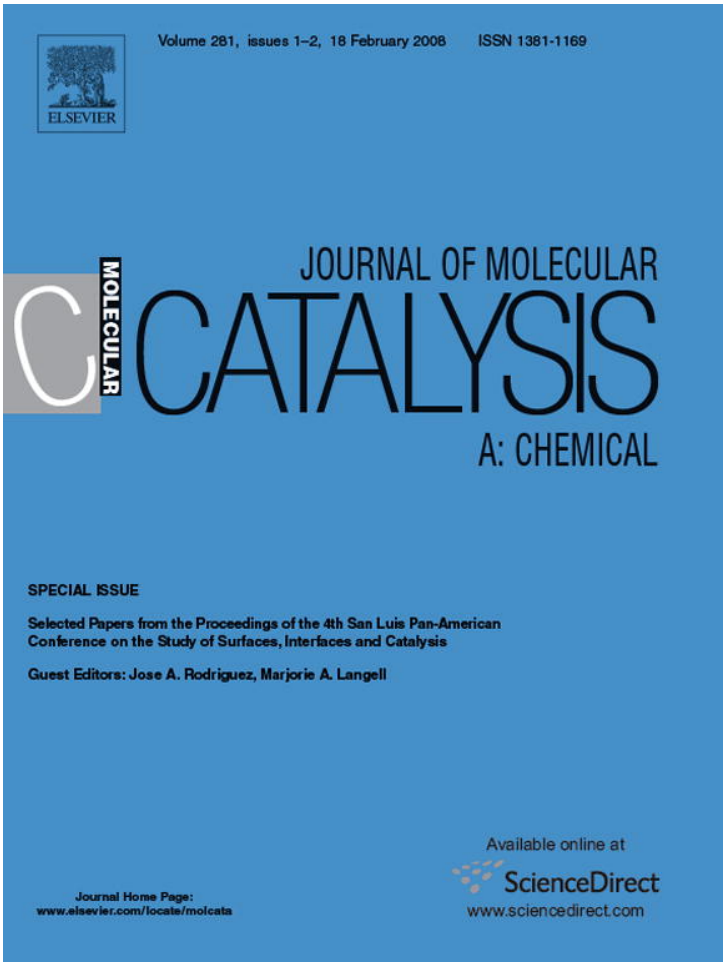

Available online at www.sciencedirect.com
ScienceDirect
Journal of Molecular Catalysis A: Chemical 281 (2008) 66–72
JOURNAL OF MOLECULAR CATALYSIS A: CHEMICAL
www.elsevier.com/locate/molcata

A comparison between the precipitation and impregnation methods for water gas shift catalysts

Amalia Luz C. Pereira [a], Guillermo José P. Berrocal [a], Sérgio G. Marchetti [b], Alberto Albornoz [c], Alexilda O. de Souza [d], Maria do Carmo Rangel [a,*]

[a] *Instituto de Química Universidade Federal da Bahia, Campus Universitário de Ondina, 40170-290 Salvador, Bahia, Brazil*
[b] *CINDECA, Facultad de Ciencias Exactas, Universidad Nacional de La Plata, 1900, 47 y 115 La Plata, Argentina*
[c] *Centro de Química, Instituto Venezolano de Investigaciones Científicas, 21827 Caracas, Venezuela*
[d] *Universidade Estadual do Sudoeste da Bahia, 45700-000 Itapetinga, Bahia, Brazil*

Available online 28 July 2007

Abstract

The precipitation and impregnation methods in the preparation of chromium-doped magnetite for water gas shift reaction (WGSR) were compared in this work. This reaction is an important step in the commercial production of highly pure hydrogen from natural gas or naphtha feedstocks. It was found that the preparation method affects both the textural and catalytic properties of chromium-doped magnetite. However, chromium was able to preserve the specific surface area during the WGSR and to delay the metallic iron production, independently of the preparation method. Chromium caused a decrease in activity per area, depending on the preparation method. This fact was assigned to its ability in making the production of Fe^{2+} species more difficult, making the catalytic sites less active, because the redox cycle of the reaction becomes more difficult. The most active catalyst was obtained by adding chromium by impregnation, which led to a large amount of total chromium in the solid and then a catalyst with high specific surface area was produced. It was showed that the catalysts can be prepared in the active phase avoiding the reduction step, before reaction.

Keywords: Chromium-doped magnetite; Hydrogen; WGSR

1. Introduction

It is well-known [1] that the preparation method of the catalysts has a strong influence on their final properties. In addition, the reactivity of the solids largely depends on the nature and on the concentration of the imperfections that can be generated during their preparation. Therefore, several factors such as concentration, pH, temperature, aging time and kind of anions can affect the final product [2]. Concerning iron oxides, several works have been carried out to state the effect of the preparation method on the properties of these catalysts [2,3]. With this goal in mind, the precipitation and impregnation methods in the preparation of chromium-doped magnetite (Fe_3O_4) were compared in this work. The characteristics of the solids produced were related to their catalytic activity in water gas shift reaction (WGSR).

In recent years, the WGSR has attracted increasing interest mainly because of its application in fuel cells [4]. By WGSR, the hydrogen production from steam reforming is increased and, most importantly, the hydrogen stream is purified by the removal of carbon monoxide which often poisons most of metallic catalysts, including the platinum electrocatalyst for fuel cells [4,5].

The water gas shift reaction: $CO + H_2O \rightleftarrows CO_2 + H_2$ has been widely investigated for different purposes, for instance, for ammonia synthesis and hydrogenation reactions. Thermodynamically, the WGSR is favored by low temperatures and excess of steam, since it is exothermic ($\Delta H = -41\ kJ\ mol^{-1}$) and reversible. However, high temperatures are required for industrial applications and thus the reaction is carried out in two steps in commercial processes: a high temperature shift (HTS) in the range of 643–693 K and a low temperature shift (LTS) at around 503 K. The HTS step is typically performed over an iron oxide-based catalyst while the LTS stage is carried out over a copper-based one. The most used HTS catalyst is chromium-doped hematite (α-Fe_2O_3), which is reduced in situ to produce magnetite (Fe_3O_4), the active phase. In this exothermic reduc-

* Corresponding author. Tel.: +55 71 3235 5166; fax: +55 71 3235 5166.
E-mail address: mcarmov@ufba.br (M.d.C. Rangel).

1381-1169/$ – see front matter © 2007 Elsevier B.V. All rights reserved.
doi:10.1016/j.molcata.2007.07.042

tion, the production of metallic iron should be avoided, since it can promote undesirable reactions such as methanation, carbon monoxide disproportionation reactions [6] and Fischer-Tropsch synthesis [7,8]. In addition, hydrogen is consumed in the process and the exothermic nature of these reactions can produce hot spots in the reactor and also the weakness and physical damage to catalyst pellets [9].

In industrial plants, the process gas (carbon monoxide and dioxide, hydrogen, methane and argon), from the reforming converters, is used to perform this reduction and large amounts of steam are added to the gas feed, in order to ensure the magnetite stability. However, this procedure increases the operational costs. Therefore, there is a demand for more stable catalysts that could avoid the iron reduction to metallic state and thus do not need an excess of steam [5]. It is expected that a catalyst prepared in the active phase can inhibit the reduction step and save energy in industrial processes. With this goal in mind, the precipitation and impregnation methods were compared, with the aim of preparing HTS catalysts in the active form.

2. Experimental

2.1. Sample preparation

In the precipitation method, an ammonium hydroxide solution (25%, m/v) was slowly added by a pump, at room temperature, to an iron nitrate (1 M) and chromium nitrate (0.1 M) solutions, previously mixed, to get the MCP sample. In the impregnation method, the ammonium hydroxide solution was added to the iron nitrate solution to produce a gel which was further impregnated with the chromium nitrate solution, for 24 h (MCI sample). The sol produced was centrifuged and the gel was washed with an ammonium acetate solution 5% (w/v) to remove the nitrate ions and to promote the sorption of acetate species, responsible for the magnetite formation [5,10]. The solid was dried at 393 K and heated under nitrogen flow (100 mL min^{-1}) at a rate of 10 K min^{-1} up to 773 K, and kept at this temperature for 2 h, to produce the catalysts. Pure magnetite was also prepared by the method described, which was used as a reference (M sample).

2.2. Catalyst characterization

The catalysts were characterized by chemical analysis, Fourier transform infrared spectroscopy (FTIR), X-ray diffraction (XRD), specific surface area measurements, temperature-programmed reduction (TPR), X-ray photoelectron spectroscopy (XPS) and Mössbauer spectroscopy.

The iron and chromium contents were determined by energy dispersive X-ray spectroscopy (EDS) in a Shimadzu model EDX-700HS equipment. The presence of acetate groups in the samples was confirmed by FTIR, using a Perkin Elmer model Spectrum One equipment, in the range of 400–4000 cm^{-1}. The XRD powder patterns of the solids were obtained in a Shimadzu model XD3A equipment, using a Cu Kα (λ = 1.5420 Å) radiation and nickel filter, with 2θ ranging from 10° to 80°. The specific surface area measurements were carried out by the BET method in a Micromeritics model TPD/TPR 2900 equipment, using a 30% N_2/He mixture. The sample was previously heated (10 K min^{-1}) up to 433 K, under nitrogen flow (60 mL min^{-1}) being kept at this temperature for additional 30 min. The TPR profiles were obtained using the same equipment. The samples (0.05 g) were reduced at a temperature ranging from 303 up to 1273 K, at 10 K min^{-1}, under a 5% H_2/N_2 mixture.

The XPS spectra were obtained with a VG Scientific spectrometer, Escalab model 220i-XL, with X-ray source, Mg Kα (1253 eV) anode and 400 W power, with a hemispheric electron analyzer. This reference was, in all cases, in good agreement with the BE of the C 1s peak, at 284.6 eV.

The Mössbauer spectra, at 298 K, were measured in transmission geometry with a 512-channel constant acceleration spectrometer. A source of ^{57}Co in an Rh matrix of nominally 50 mCi was used. Velocity calibration was performed against a 12 μm-thick α-Fe foil. All isomer shifts (δ) are referred to this standard at room temperature. The spectra were folded to minimize geometric effects, being evaluated using a commercial computer fitting program named Recoil.

2.3. Catalysts evaluation

The catalysts were evaluated using 0.2 cm^3 of powder 100 mesh size and a fixed bed microreactor operating at 643 K, 1 atm and WHSV = 12,000 h^{-1}, for 6 h. A gas mixture (10% CO, 10% CO_2, 60% H_2 and 20% N_2) and a steam to gas molar ratio of 0.6 were used. These conditions were chosen to achieve a 10% conversion (far from the equilibrium value, 46%) using a commercial catalyst (chromium-doped hematite) and also to avoid any diffusion effect. After each experiment, the reactor with the catalyst was cooled under nitrogen (with traces of oxygen) until reaching room temperature, to avoid the pyrophoric effects [4,11]. The spent catalysts were analyzed by XRD, specific surface area measurements, Mössbauer spectroscopy and XPS.

3. Results and discussion

The FTIR spectra of the samples before heating, shown in Fig. 1(a), confirmed the presence of acetate groups by the absorption bands at 1550 and 1430 cm^{-1} [12]. The spectra also show bands at 3400 and 1380 cm^{-1}, assigned to hydroxyl and nitrate groups, respectively [13,14], besides a broad Fe–O absorption band below 800 cm^{-1} [15]. After heating at 773 K under nitrogen, for 2 h, the bands related to acetate and nitrate groups disappeared and a band at 570 cm^{-1} assigned to magnetite [16] appeared, as shown in Fig. 1(b). The chromia characteristic bands [16] and the typical bands of chromates [17] were not detected, in agreement with previous works [10,18].

In accordance with these results, the X-ray diffractograms showed that during heating the solids produced magnetite (JCPDF 88-0315) and no other phase was found, regardless the preparation method and the presence of chromium, as shown in Fig. 2(a). After WGSR, the X-ray patterns did not change

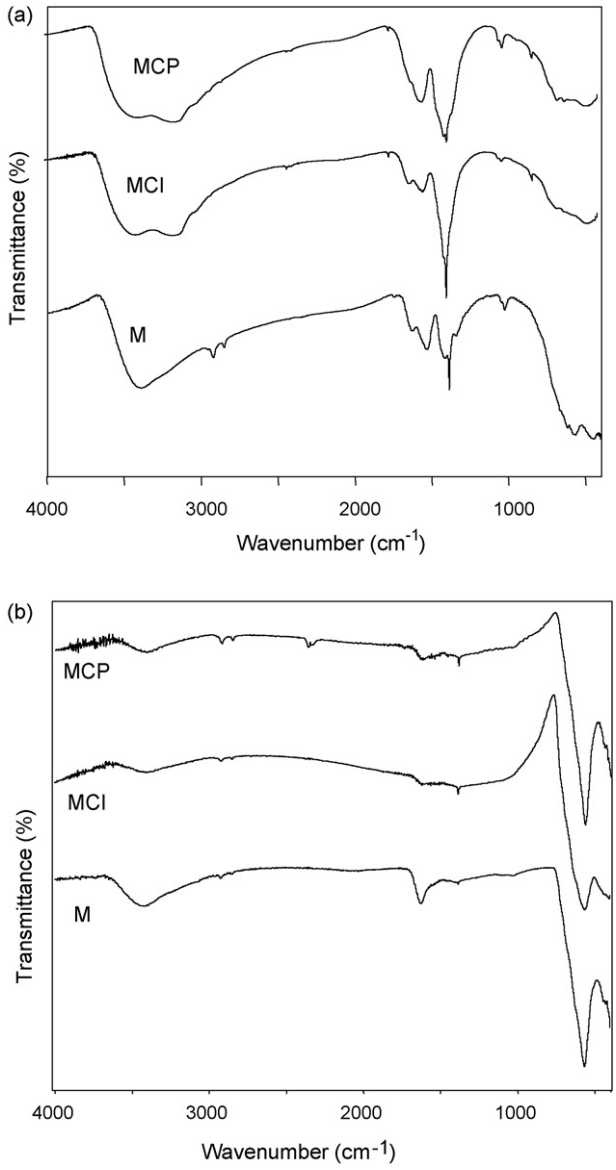

Fig. 1. FTIR spectra of the samples (a) before and (b) after heating under nitrogen flow. M, magnetite; C, chromium; P, precipitation; I, impregnation.

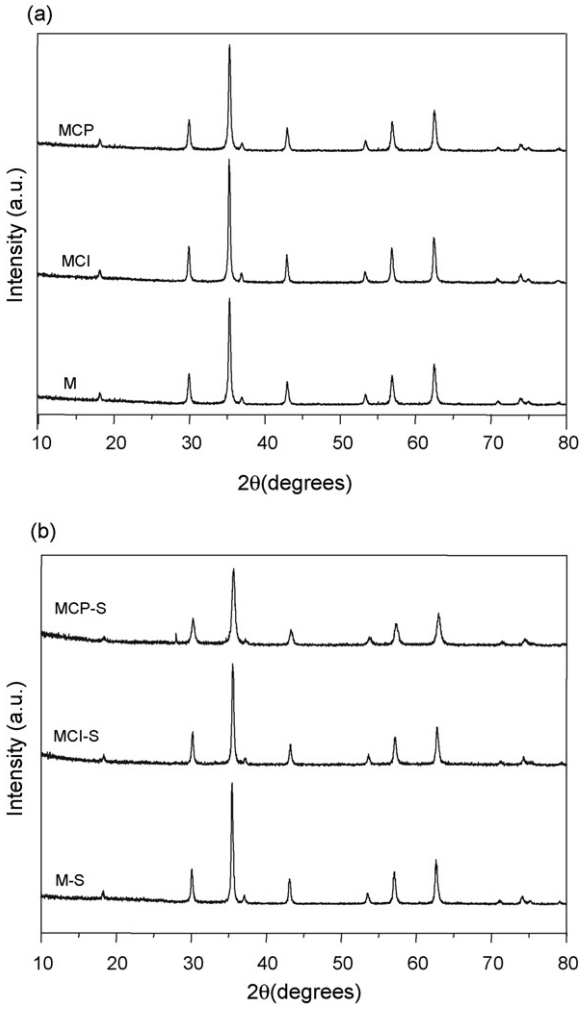

Fig. 2. X-ray diffractograms of the (a) fresh and of the (b) spent catalysts. M, magnetite; C, chromium; P, precipitation; I, impregnation.

(Fig. 2(b)), indicating that the catalysts were stable during reaction.

The TPR of pure iron oxide showed a curve with two small reduction peaks between 543 and 673 K (Fig. 3), both attributed to the reduction of Fe^{3+} to Fe^{2+} species; they can be related to the reduction of a maghemite layer produced on the solids due to air exposition. A high temperature peak, in the range of 723–1043 K, is assigned to the reduction of Fe^{2+} to Fe^{0} species [19]. The additional peak at 1138 K can be related to the reduction of the residual iron oxide in the center of the particles, which was reduced at higher temperatures. It is well-known [20,21] that the reduction of iron oxide proceeds through a surface-controlled process; once a thin layer of iron oxide with lower oxidation state (wustite, metallic) is formed on the surface, it changes to diffusional control. Therefore, this residual core does not easily access the reducing gas and thus is reduced at higher temperature where the diffusional process is faster. The addition of

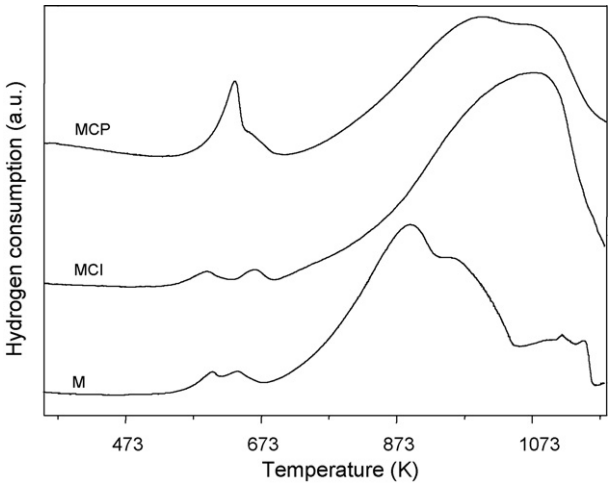

Fig. 3. TPR profiles of the catalysts. M, magnetite; C, chromium; P, precipitation; I, impregnation.

Table 1
Specific surface areas of the catalysts before (Sg) and after the WGSR (Sg^*)

Sample	Sg ($m^2\ g^{-1}$)	Sg^* ($m^2\ g^{-1}$)
MCP	20	22
MCI	29	28
M	13	11

M, magnetite; C, chromium; P, precipitation; I, impregnation.

chromium to magnetite did not affect its reduction profile, but shifted the peaks to high temperatures. It means that chromium made the production of metallic iron more difficult, suggesting that it can delay this process during WGSR, in agreement with previous works [22].

The results of the specific surface area measurements of the solids are shown in Table 1. The chromium-doped samples showed specific surface areas higher than magnetite, regardless the preparation method, showing the role of chromium as textural promoter, in accordance with previous works [8,11]. In addition, the impregnated sample showed higher specific surface area than the precipitated one. After WGSR, the solids did not show changes in the specific surface areas, indicating that the solids were stable during reaction.

A typical Fe 2p core-level spectrum of the catalysts before reaction is shown in Fig. 4(a). A similar profile was obtained with the spent catalysts. The Fe^{3+} and Fe^{2+} species can be identified by two peaks at around 710.0 and 711.0 eV and a satellite structure located at the high binding energy side [23]. Fig. 4(b) illustrates a typical Cr 2p core-level spectrum of the catalysts before WGSR, which did not change during reaction. The Cr^{3+} species were identified by a peak at around 576.0 eV and a satellite structure located at the high binding energy side [23].

In all cases, the amount of chromium on the surface was higher than in the bulk, as noted by comparing the results of EDS (bulk) and XPS (surface), shown in Table 2, in accordance with previous works [8,24–26]. Therefore, the role of chromium in delaying sintering can be assigned to its action as a spacer on the surface, making the particles apart, as proposed by other authors [8,24]. During the water gas shift reaction, some chromium had migrated from the surface but it did not cause a significant change in specific surface areas. It suggests that chromium also plays a role in the bulk, as noted previously for aluminum [27,28] and chromium-doped iron oxide [29,30]. In fact, Edwards et al. [29] showed that Cr^{3+} (d^3) goes into the magnetite lattice and occupies the octahedral sites because of its high crystal field stabilization, in contrast with the Fe^{3+} ion (d^5) which does not have any preferred site. In this case, chromium is supposed to cause strains in the lattice, during the spinel formation, and then shifts the equilibrium particle size towards smaller particles, since it decreases the strain to the surface effects ratio.

Table 2
Catalysts composition in the bulk and on the surface

Sample	Bulk molar ratio Cr/Fe	Surface molar ratio Cr/Fe		Surface ratio Fe^{2+}/Fe^{3+}	
		Fresh	Spent	Fresh	Spent
MCP	0.090	0.199	0.077	1.56	0.43
MCI	0.120	0.334	0.177	2.00	0.34
M	–	–	–	1.09	0.98

M, magnetite; C, chromium; P, precipitation; I, impregnation.

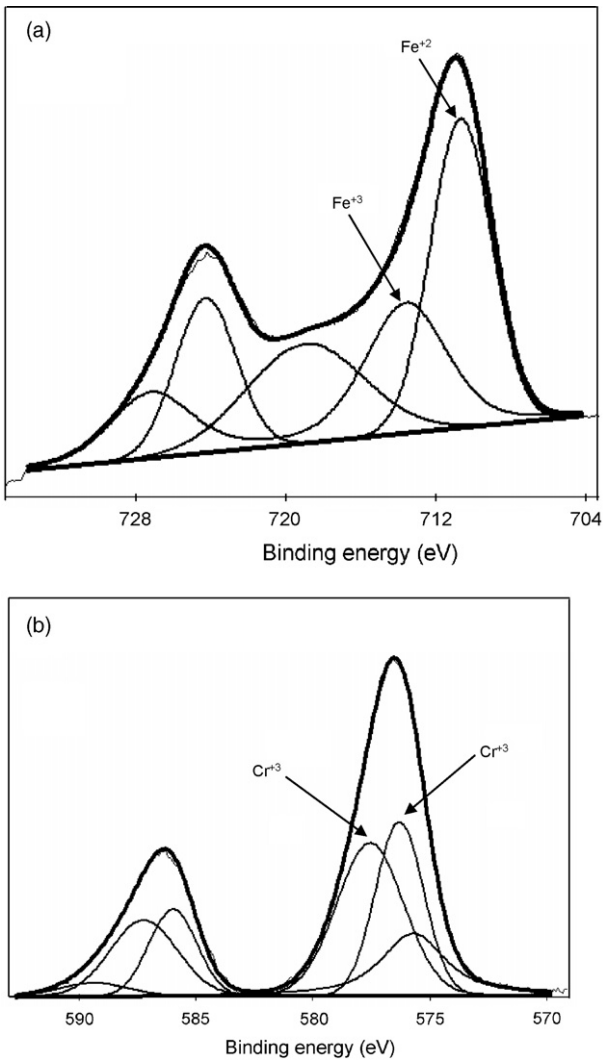

Fig. 4. (a) Fe2p core-level spectra and (b) Cr2p core level for the MCP sample (chromium-doped magnetite prepared by precipitation).

It can also be noted that the impregnation method led to the production of solids with higher amounts of chromium on the surface, as compared to the precipitated one. This method also led to a higher total amount of chromium in the solid, a fact which can explain the higher specific surface area of the MCI sample. This can be related to the lower rates of precipitation of chromium compounds as compared to the iron ones. It is well-known [31–36] that Fe^{3+} and Cr^{3+} ions undergo hydrolysis and polymerization in aqueous medium, as the pH increases. Both ions exist as simple aquo-ions and form octahedral complexes. As the Fe^{3+} cation ($3d^5$) does not show any crystal field stabilization in octahedral symmetry, the rates of hydrolysis and of polymerization are higher than those of the Cr^{3+} one ($3d^3$) which exhibits a high crystal field stabilization in the same symmetry. Therefore, chromium cation is the least

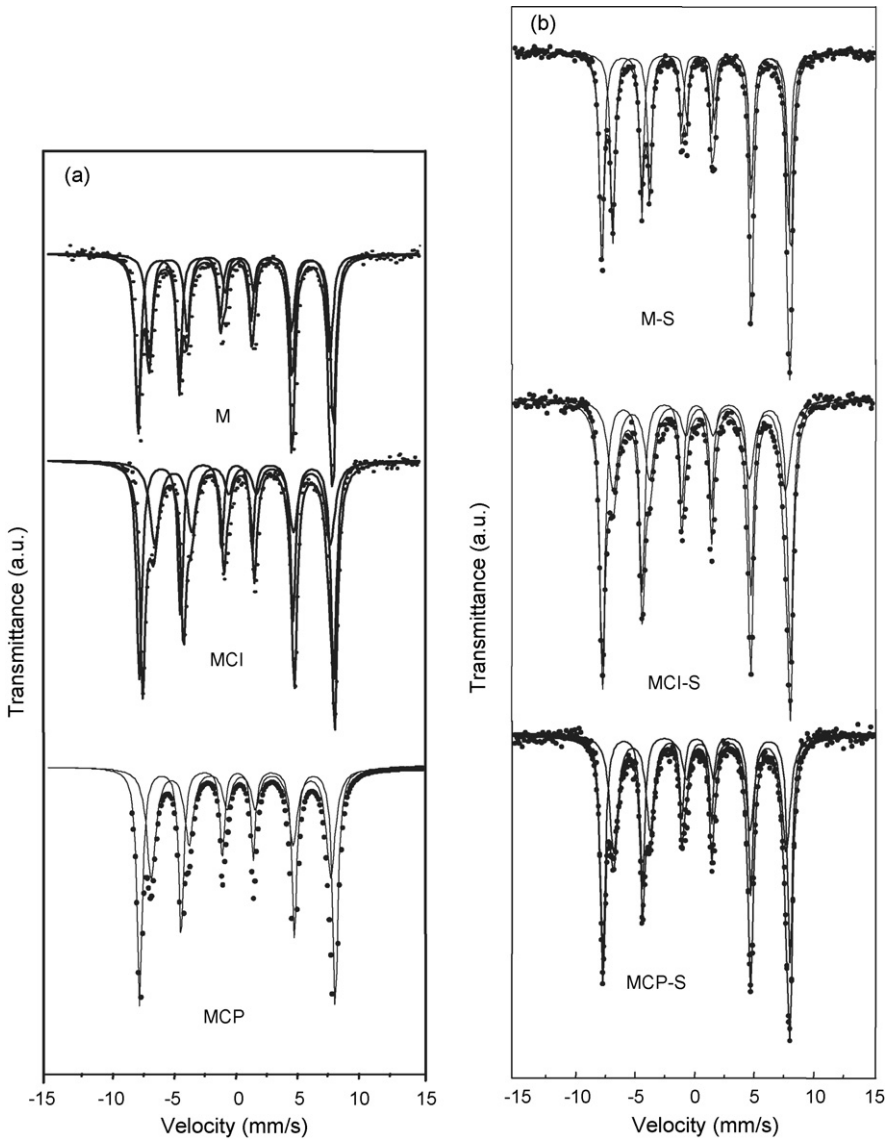

Fig. 5. Mössbauer spectra at 298 K of the (a) fresh and (b) spent catalysts. M, magnetite; C, chrome; P, precipitation; I, impregnation; S, spent.

hydrolyzed since it is the most crystal field-stabilized one and then the OH^- species are supposed to produce a weaker field than water. As the olation reaction rates slow down as the crystal field stabilization increases, a decrease of the reactivity of the chromium cation towards the ligand exchange is expected. In agreement, the rate of dimerization of the $[Fe(OH)(OH_2)_5]^{2+}$ ion is $k = 450\,L\,mol^{-1}$ (25 °C) while the rate of dimerization of the $[Cr(OH)(OH_2)_5(C_2O_4)_2]^{2+}$ is $k = 10^{-5}\,L^2\,mol^{-2}\,s^{-1}$ [31]. In the present work, one can suppose therefore that in the preparation conditions the iron compounds precipitated in a larger extension than the chromium ones. On the other hand, during impregnation (24 h) there was enough time for most of chromium to be sorbed on the particles.

The Fe^{2+}/Fe^{3+} molar ratios on the surface are also shown in Table 2. It can be seen that chromium caused an increase of these values and this effect was more pronounced for the impregnated sample. After reaction, however, the opposite was noted and the chromium-doped catalysts showed the lowest values. A large decrease of the relative amounts of these species was noted after reaction, in the case of chromium-doped catalysts.

The Mössbauer spectrum of pure magnetite (Fig. 5(a)) was fitted with two sextets whose hyperfine parameters correspond to Fe^{3+} in tetrahedral sites (A sites) and $Fe^{\text{“}2.5+\text{”}}$ in octahedral sites (B sites) of Fe_3O_4 (Tables 4 and 5) [37]. The chromium addition to magnetite (MCP and MCI samples) produced a decrease in the hyperfine magnetic fields in both sites. This effect can be attributed to the replacement of iron ions by chromium ones.

Table 3
Catalytic activity (a) and activity per area (a/Sg^*) of the catalysts in WGSR

Sample	$a \times 10^6$ (mol g^{-1} s^{-1})	$a/Sg^* \times 10^7$ (mol m^{-2} s^{-1})
MCP	2.4	1.1
MCI	5.0	1.7
M	2.4	2.2

M, magnetite; C, chromium; P, precipitation; I, impregnation.

Table 4
Mössbauer parameters at 298 K of the fresh catalysts

Species	Parameters	MCP	MCI	M
Fe_3O_4 A site	H_A (T)	48.9 ± 0.1	49.0 ± 0.1	49.4 ± 0.1
	$\delta_($ (mm s^{-1})	0.32 ± 0.01	0.32 ± 0.01	0.31 ± 0.01
	$2\varepsilon_A$ (mm s^{-1})	−0.03 ± 0.01	−0.02 ± 0.01	−0.02 ± 0.01
	%	56 ± 3	58 ± 3	60 ± 3
Fe_3O_4 B site	H_B (T)	44.9 ± 0.1	44.9 ± 0.1	45.7 ± 0.1
	$\delta_($ (mm s^{-1})	0.59 ± 0.01	0.56 ± 0.01	0.64 ± 0.01
	$2\varepsilon_B$ (mm s^{-1})	−0.01 ± 0.02	−0.01 ± 0.03	0.01 ± 0.01
	%	44 ± 3	42 ± 3	40 ± 2
	B/A ratio	0.79 ± 0.07	0.72 ± 0.06	0.67 ± 0.05

M, magnetite; C, chromium; P, precipitation; I, impregnation. H: hyperfine magnetic field in Teslas; δ: isomer shift (all the isomer shifts are referred to α-Fe at 298K); 2ε: quadrupole shift; A: tetrahedral sites; B: octahedral sites.

Table 5
Mössbauer parameters at 298 K of spent (S) catalysts

Species	Parameters	MCP-S	MCI-S	M-S
Fe_3O_4 A site	H_A (T)	48.8 ± 0.1	49.1 ± 0.1	49.3 ± 0.1
	$\delta_($ (mm s^{-1})	0.31 ± 0.01	0.31 ± 0.01	0.30 ± 0.01
	$2\varepsilon_A$ (mm s^{-1})	−0.02 ± 0.01	−0.01 ± 0.01	−0.02 ± 0.01
	%	52 ± 3	60 ± 3	53 ± 2
Fe_3O_4 B site	H_B (T)	45.0 ± 0.1	45.0 ± 0.2	45.8 ± 0.1
	$\delta_($ (mm s^{-1})	0.61 ± 0.01	0.55 ± 0.02	0.65 ± 0,01
	$2\varepsilon_B$ (mm s^{-1})	−0.01 ± 0.02	−0.02 ± 0.03	0.01 ± 0,01
	%	48 ± 3	40 ± 3	47 ± 2
	B/A ratio	0.92 ± 0.08	0.67 ± 0.06	0.89 ± 0.05

M, magnetite; C, chromium; P, precipitation; I, impregnation. H: hyperfine magnetic field in Teslas; δ: isomer shift (all the isomer shifts are referred to α-Fe at 298 K); 2ε: quadrupole shift; A: tetrahedral sites; B: octahedral sites.

This decrease was more pronounced in B sites, indicating that chromium ions entered preferentially into these sites. Notwithstanding, within the experimental errors, the B/A population ratio is the same for all fresh samples. Although it is well-known that to estimate unambiguously the populations of A and B sites it is necessary to do measurements at low temperatures [38], the present results are adequate for comparative purposes. It was also noted that the amount of Fe^{2+} and Fe^{3+} species depends on the preparation method. For the spent MCP and M samples (Fig. 5(b)) the B/A ratio has been increased about 20% as compared to the fresh solids, while for the MCI sample this relation remains constant.

It has been pointed out [39] that magnetite goes on slow oxidation at low temperatures producing maghemite or hematite depending on its preparation method. Therefore, the production of an oxidized iron oxide on the magnetite particles is expected. In the present work, this layer was detected by TPR on fresh catalysts and probably was also present on the spent ones. Because of this, the XPS and Mössbauer experiments were used for comparison among samples exposed to the same conditions. The Fe^{2+}/Fe^{3+} surface ratio remains the same during reaction for the M sample and thus the re-oxidation due to air exposition can be considered the same for all samples; consequently, the decrease of the Fe^{2+}/Fe^{3+} surface ratio for the MCP and MCI samples during reaction should not be attributed to air exposition and can be related to chromium presence. In addition, Mössbauer spectroscopy is less sensitive to the surface characteristics (except when the crystallites are extremely small) than XPS and then the agreements between these two techniques shows that the re-oxidation of the samples due to air exposition can be considered negligible for comparative purposes.

As expected, chromium increased the activity of the catalysts as shown in Table 3. The preparation method strongly affected the activity of the chromium-doped samples, which increased in the order: MCP < MCI. In both cases, chromium caused an increase in specific surface area, but a decrease in activity per area. The decrease in the activity per area can be assigned to the chromium ability in making the production of Fe^{2+} species more difficult, as shown by the Mössabuer spectroscopy and XPS results. This can decrease the activity of the catalytic sites, by making the iron redox cycle more difficult during WGSR. It is largely accepted that the WGSR on iron-based catalysts occurs by the regenerative mechanism, according to which the surface undergoes successive oxidation and reduction cycles by oxygen and water and carbon monoxide [8]. For the precipitated sample, it resulted in a large decrease in the activity per area and a catalyst with the same activity as magnetite was obtained, due to the textural action of chromium. On the other hand, for the impregnated catalyst, the decrease in the activity per area was not enough to overcome the increased activity due to the higher specific surface area and a more active catalyst was produced. Fig. 6 shows the activity of the catalysts as a function of time. It

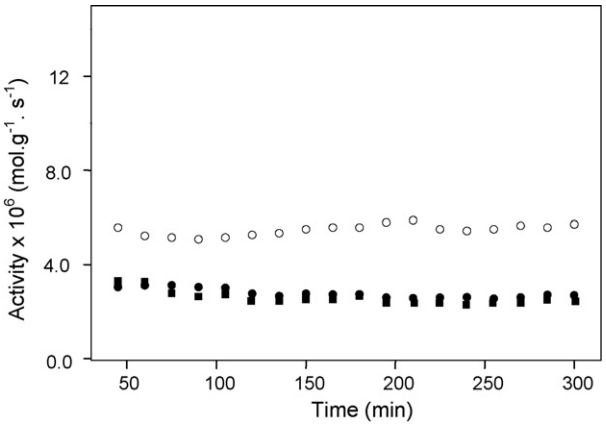

Fig. 6. Activity of the catalysts as a function of time. (●) MCP sample; (◯) MCI sample; (■) M sample. M, magnetite; C, chromium; P, precipitation; I, impregnation.

can be seen that all the samples were stable during the reaction time.

4. Conclusions

The use of the precipitation and impregnation methods for preparing chromium-doped magnetite leads to catalysts with different textural and catalytic properties towards the water gas shift reaction. However, chromium is able to preserve the specific surface areas during WGSR and to delay the metallic iron production, regardless the preparation method.

Chromium also causes a decrease in activity per area, depending on the preparation method. This fact can be assigned to its ability in making the production of Fe^{2+} species more difficult and then decreasing the activity of the catalytic sites, during the redox cycle of the reaction. The most active catalyst can be obtained by adding chromium by impregnation, which leads to a large amount of total chromium in the solid and then a catalyst with high specific surface area is produced. Chromium is believed to act both in the bulk and on the surface preventing sintering.

Moreover, it was confirmed that it is possible to prepare the catalysts in the active phase avoiding the reduction step.

Acknowledgements

ALCP and GJPB acknowledge CNPq for their graduate fellowships. The authors acknowledge CNPq, FAPESB and FINEP for the financial support.

References

[1] M. Shimokawabe, R. Furuichi, T. Ishii, Thermochim. Acta 21 (1977) 373–384.
[2] E. Matijevic, P. Sheider, J. Colloid Interface Sci. 63 (1978) 509–524.
[3] M.C. Rangel, M.S. Santos, A. Albornoz, Stud. Surf. Sci. Catal. 162 (2006) 753–760.
[4] G. Grubert, S. Kolf, M. Baerns, I. Vauthey, D. Farrusseng, A.C. van Veen, C. Mirodatos, E.R. Stobbe, P.D. Cobden, Appl. Catal. A: Gen. 306 (2006) 17–21.
[5] I. Lima Júnior, J.M. Millet, M. Aouineb, M.C. Rangel, Appl. Catal. A: Gen. 283 (2005) 91–98.
[6] St.G. Christoskova, M. Stoyanova, M. Georgieva, Appl. Catal. A: Gen. 208 (2001) 235–242.
[7] T. Tabakova, V. Idakiev, K. Tenchev, F. Boccuzzi, M. Manzoli, A. Chiorino, Appl. Catal. B: Environ. 63 (2006) 94–103.
[8] M.V. Twigg, L. Lloyd, D.E. Ridler, Catalyst Handbook, Manson Publishing Ltd., London, 1996.
[9] C. Rhodes, G.T. Hutchings, A.M. Ward, Catal. Today 23 (1995) 43–58.
[10] M.C. Rangel, F. Galembeck, J. Catal. 145 (1994) 364–371.
[11] A.V. Krylova, G.A. Ustimenko, N.V. Nefedova, T.M. Peev, N.S. Torocheshnikov, Appl. Catal. 20 (1986) 205–213.
[12] R. Silverstein, G.C. Basslerand, T.C. Morrill, Spectrometry Identification of Organic Compounds, Wiley, New York, 1991.
[13] J.D. Russell, Clay Miner. 14 (1979) 109–114.
[14] R.A. Niquist, R.O. Kagel, Infrared Spectra of Inorganic Compounds, Academic Press, Orlando, 1971.
[15] U. Scwertmann, W.R. Fischer, Geoderma 10 (1973) 237–247.
[16] N.T. McDevitt, W.L. Baun, Spectrochim. Acta 20 (1964) 799–808.
[17] J.A. Campbell, Spectrochim. Acta 21 (1965) 1333–1343.
[18] M.C. Rangel, R.M. Sassaki, F. Galembeck, Catal. Lett. 33 (1995) 237–254.
[19] J.C. González, M.G. González, M.A. Laborde, N. Moreno, Appl. Catal. 20 (1986) 3–13.
[20] T. Wiltowski, K. Piotrowski, H. Lorethova, L. Stonawski, K. Mondal, S.B. Lalvani, Chem. Eng. Proc. 44 (2005) 775–783.
[21] K. Piotrowski, K. Mondal, H. Lorethova, L. Stonawski, T. Szymański, T. Wiltowski, Int. J. Hydrogen Energy 30 (2005) 1543–1554.
[22] S. Natesakhawat, X. Wang, L. Zhang, U.S. Ozkan, J. Mol. Catal. A 260 (2006) 82–94.
[23] C.D. Wagner, W.M. Riggs, L.E. Davis, J.F. Moulder, G.E. Muilenberg, Handbook of X-Ray Photoelectron Spectroscopy, Perkin-Elmer Corporation, Eden Prairie, 1978.
[24] G.C. Chinchen, R.H. Logan, M.S. Spencer, Appl. Catal. 12 (1984) 97–103.
[25] M.C. Kung, H.H. Kaung, Surf. Sci. 104 (1981) 253–269.
[26] C. Rhodes, G.T. Hutchings, Phys. Chem. Chem. Phys. 5 (2003) 2719–2723.
[27] H. Topsoe, J.A. Dumesic, M. Boudart, J. Catal. 28 (1978) 477–488.
[28] M.C. Rangel, G.C. Araújo, Catal. Today 62 (2000) 201–207.
[29] M.A. Edwards, D.M. Whittle, C. Rhodes, A.M. Ward, D. Rohan, M.D. Shannon, G.J. Hutchings, C.J. Kiely, Phys. Chem. Chem. Phys. 4 (2002) 3902–3908.
[30] M. Robbins, G.K. Wertheim, R.C. Sherwood, D.N.E. Buchanan, J. Phys. Chem. Solids 32 (1971) 717–729.
[31] J.P. Punt, in: J. Burguess (Ed.), Metal Ions in Aqueous Solution, Benjamin, New York, 1965, pp. 45–54.
[32] C.F. Baes Jr., R.E. Mesmer, The Hydrolysis of Cations, Wiley, New York, 1976.
[33] J. Burguess, in: J. Burguess (Ed.), Metal Ions in Aqueous Solution, Benjamin, New York, 1965, pp. 269–309.
[34] J. Livage, M. Henry, C. Sanchez, Prog. Sol. State Chem. 18 (1988) 259–341.
[35] H. Wendt, Inorg. Chem. 8 (1969) 1527–1528.
[36] M.A. Blesa, E. Matijevic, Adv. Colloid Interface Sci. 29 (1989) 173–221.
[37] R.E. Vandenberghe, E. De Grave, G.J. Long, F. Grandjean, Mössbauer Spectroscopy Applied to Inorganic Chemistry, Plenum Press, New York, 1989.
[38] N. Viart, G. Pourroy, J.M. Greneche, D. Niznansky, J. Hommet, Eur. Phys. J. AP: 12 (1) (2000) 37–46.
[39] P.S. Sidhu, R.J. Gilkes, A.M. Posner, J. Inorg. Nucl. Chem. 39 (1977) 1953–1958.